U.S. Army
Research Institute of
Environmental Medicine
Natick, Massachusetts

TECHNICAL REPORT NO. T19-04
DATE January 2019

EFFECTS OF DIFFERENT BODY ARMOR CONFIGURATIONS ON BODY HEAT LOSS DURING EXPOSURE TO EXTREME COLD ENVIRONMENTS USING THE FINITE ELEMENT METHOD

United States Army
Medical Research & Materiel Command

DISCLAIMER

The opinions or assertions contained herein are the private views of the author(s) and are not to be construed as official or reflecting the views of the Army or the Department of Defense. The investigators have adhered to the policies for protection of human subjects as prescribed in 32 CFR Part 219, Department of Defense Instruction 3216.02 (Protection of Human Subjects and Adherence to Ethical Standards in DoD-Supported Research) and Army Regulation 70-25.

USARIEM TECHNICAL REPORT T19-04

EFFECTS OF DIFFERENT BODY ARMOR CONFIGURATIONS ON BODY HEAT LOSS DURING EXPOSURE TO EXTREME COLD ENVIRONMENTS USING THE FINITE ELEMENT METHOD

Michael P. Castellani
Timothy P. Rioux
Julio A Gonzalez
Adam W. Potter
Xiaojiang Xu

Biophysics and Biomedical Modeling Division

January 2019

U.S. Army Research Institute of Environmental Medicine
Natick, MA 01760-5007

REPORT DOCUMENTATION PAGE

Form Approved
OMB No. 0704-0188

PLEASE DO NOT RETURN YOUR FORM TO THE ABOVE ADDRESS.

1. REPORT DATE *(DD-MM-YYYY)*	2. REPORT TYPE	3. DATES COVERED *(From - To)*
15-01-2019	Technical Report	2018-2019

4. TITLE AND SUBTITLE

EFFECTS OF DIFFERENT BODY ARMOR CONFIGURATIONS ON BODY HEAT LOSS DURING EXPOSURE TO EXTREME COLD ENVIRONMENTS USING THE FINITE ELEMENT METHOD

5a. CONTRACT NUMBER

5b. GRANT NUMBER

5c. PROGRAM ELEMENT NUMBER

6. AUTHOR(S)

Michael P. Castellani
Timothy P. Rioux
Julio A Gonzalez
Adam W. Potter
Xiaojiang Xu

5d. PROJECT NUMBER

5e. TASK NUMBER

5f. WORK UNIT NUMBER

H

7. PERFORMING ORGANIZATION NAME(S) AND ADDRESS(ES)

Biophysics and Biomedical Modeling Division
U.S. Army Research Institute of Environmental Medicine
Building 42 - 10 General Greene Ave
Natick, MA 01760

8. PERFORMING ORGANIZATION REPORT NUMBER

9. SPONSORING/MONITORING AGENCY NAME(S) AND ADDRESS(ES)

U.S. Army Medical Research and Materiel Command,
Fort Detrick, MD 21702

10. SPONSOR/MONITOR'S ACRONYM(S)

11. SPONSOR/MONITOR'S REPORT NUMBER(S)

T19-04

12. DISTRIBUTION/AVAILABILITY STATEMENT

Approved for public release; distribution unlimited

13. SUPPLEMENTARY NOTES

14. ABSTRACT

One-dimensional models containing a combination of human skin, clothing, body armor, and a cold-weather environment were created in COMSOL Multiphysics® (Burlington, MA) software. The models created were then used to conduct heat transfer simulations using finite element analysis. The goal of this project was to determine the magnitude that the composite material of the ballistic protection plates within body armor insulate the Soldier or exacerbate heat loss in cold-weather environments. Three different models were created: (1) a skin and clothing system, M1; (2) a skin, clothing, and body armor system without the Enhanced Small Arms Protective Insert (ESAPI) plates, M2; and (3) a skin, clothing, and body armor system including the ESAPI plates, M3. It was assumed that the temperature of the skin (Ts) was 31°C and that the air temperature was between 0 and -50°C. Heat transfer properties for the skin were obtained through COMSOL Multiphysics®.

15. SUBJECT TERMS

biophysics; clothing; predictive modeling; thermoregulation; finite element analysis; heat exchange

16. SECURITY CLASSIFICATION OF:			17. LIMITATION OF ABSTRACT	18. NUMBER OF PAGES	19a. NAME OF RESPONSIBLE PERSON
a. REPORT	b. ABSTRACT	c. THIS PAGE			Adam W. Potter
Unclassified	Unclassified	Unclassified	Unclassified	28	19b. TELEPHONE NUMBER *(Include area code)* 508-233-4735

Reset

Standard Form 298 (Rev. 8/98)
Prescribed by ANSI Std. Z39.18

TABLE OF CONTENTS

LIST OF FIGURES

LIST OF TABLES

ACKNOWLEDGMENTS

The authors would like to thank Ms. Kristine Isherwood, Ms. Deirdre Townes, Mr. Gary Proulx, and Ms. Peggy Auerbach of Natick Solider Research, Development and Engineering Center (NSRDEC) for their support, thoughtful discussions and for providing thermal properties of the body armor materials. We would also like to thank Dr. Scott Montain and Dr. John Castellani for their critical review of this technical report.

EXECUTIVE SUMMARY

One-dimensional models containing a combination of human skin, clothing, body armor, and a cold-weather environment were created in COMSOL Multiphysics® (Burlington, MA) software. The models created were then used to conduct heat transfer simulations using finite element analysis. The goal of this project was to determine the magnitude that the composite material of the ballistic protection plates within body armor insulate the Soldier or exacerbate heat loss in cold-weather environments. Three different models were created: (1) a skin and clothing system, M1; (2) a skin, clothing, and body armor system without the Enhanced Small Arms Protective Insert (ESAPI) plates, M2; and (3) a skin, clothing, and body armor system including the ESAPI plates, M3. It was assumed that the temperature of the skin (T_s) was 31°C and that the air temperature was between 0 and -50°C. Heat transfer properties for the skin were obtained through COMSOL Multiphysics®. Material properties for the clothing, body armor, and ESAPI were obtained from biophysical assessments performed at the US Army Research Institute of Environmental Medicine and the Natick Soldier Research, Development, and Engineering Command or estimated based from the published literature.

The simulations performed indicate that the initial temperatures of body armor at start of simulation (i.e., the temperature when the body armor is donned) affects body heat loss during initial periods of exposure to cold environments due to the thermal mass possessed by the armor. This confounding effect can persist up to 3 hours, depending on time for the armor to reach operating temperatures. The thermal mass of the body armor will reduce body heat loss during transition to cold environments when the initial temperature of body armor is near indoor room temperatures. However, when the armor's initial temperature is nearer that of cool/cold outside environmental temperatures (body armor is stored outside or inside with no heating), the body armor will initially increase the rate of body heat loss before and become a heat sink. Thus, storing body armor in warm storage areas whenever possible will help prevent accelerated heat loss during initial exposure periods to cold environments.

INTRODUCTION

During cold-weather missions, Soldiers wear cold weather ensembles with heavy insulation to protect body temperature. In certain scenarios, body armor may be worn. This leads to the question of how the temperature and thermal mass of the body armor will affect heat transfer and body temperature retention in cold weather operations. Besides having a thermal mass that can accelerate or decelerate heat loss to the environment, its mass and dimensions can lead to compression of the cold weather ensembles themselves and thereby reduce its insulation and level of cold protection.

Heat transfer from the human skin to the environment is complex and varies at different areas on the body. Conduction occurs between contacting surfaces of different components. Radiation exists between the exterior clothing layer and the environment as well as within the still air layers of the clothing system, including the thermal contact resistance of interacting solid materials due to imperfect surface contact. Finally, convection is a major source of heat transfer between the exterior layer and the environment. The combination of these heat transfer mechanisms determines the total heat loss from a person to cold environments

The purpose of this project was to predict the magnitude of heat transfer that will occur when the Enhanced Small Arms Protective Insert (ESAPI) plate combined with the Improved Outer Tactical Vest (IOTV) is worn with typical cold weather ensembles in cold and extreme cold environments and the temperature of the ESAPI is manipulated. A simulation approach was used to simulate heat flux changes, with heat loss calculated using COMSOL Multiphysics® (Burlington, MA) software. This software program uses finite element analysis to approximate differential equations. A mesh of the human torso was used for the simulations, and starting temperatures of the armor and the wind and ambient temperatures were varied to predict the impact of body armor on heat loss under a variety of cold weather conditions.

METHODS

PHYSICAL MODELS

Cold weather ensembles designed by NSRDEC for wear during combat situations are:

(1) Light-weight cold weather undershirt/drawers and extreme cold wet jacket/trousers;
(2) (1) + IOTV without ESAPI;
(3) (1) + IOTV with the ESAPI.

Three physical models were created to represent the interaction between the skin and these three ensembles (figure 1 and 2). The 3 models were:
(1) Skin and clothing (M1);
(2) Skin, clothing, and IOTV without ESAPI (M2);
(3) Skin, clothing, and IOTV with the ESAPI (M3).

M1 represents a basic scenario where only a cold weather ensemble is worn. M2 represents the scenario where a cold weather ensemble is worn along with body armor without the ESAPI insert. M3 represents scenarios where cold weather ensembles are combined with body armor while wearing the ESAPI insert. It was assumed that heat transfer properties in each layer were uniform.

The specific body armor analyzed in this project consisted of the Improved Outer Tactical Vest (IOTV) and the Enhanced Small Arms Protective Insert (ESAPI) plate. The cold weather clothing ensemble modeled in this project consisted of levels 1 (silk weight underwear) and 5 (soft shell outer layer) from the third generation Extended Cold Weather Clothing System (ECWCS). More clothing is typically worn in cold weather environments, but it is typically doffed during missions because it restricts movement. Figure 1 illustrates the clothing ensemble and armor used on the thermal manikin.

Figure 1: Images of the outer layer of the clothing worn that was used in the simulations. Left: extreme cold wet jacket and trousers. Right: extreme cold wet jacket and trousers with IOTV.

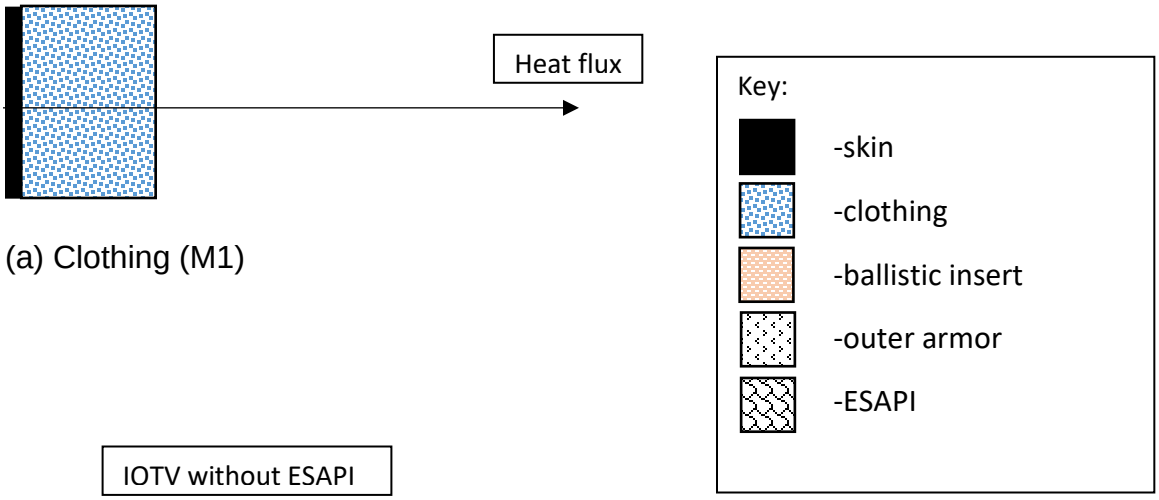

(a) Clothing (M1)

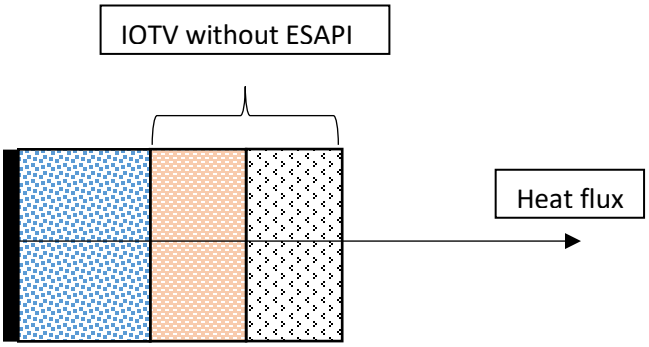

(b) Clothing, Ballistic insert, Outer armor (M2)

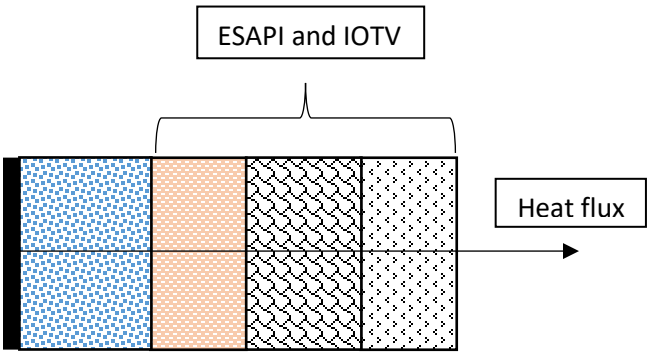

(c) Clothing, Ballistic insert, ESAPI, Outer armor (M3)

Figure 2. Illustrations of clothing for (a) M1, (b) M2, and (c) M3 models

HEAT TRANSFER PHYSICS

The heat transfer equation was used to describe temperature changes produced by the simulations. Since the simulations performed were one dimensional, the equation became:

$$\rho C_p \frac{\partial T}{\partial t} = \lambda \frac{\partial^2 T}{\partial x^2} \quad \text{Eq. 1}$$

where ρ is the density (kg·m^{-3}), C_p is the specific heat (J·kg^{-1}·K^{-1}), T is temperature (°C), t is time (s), λ is the thermal conductivity (W·m^{-1}), and x is the spatial variable (m). The heat flux, q (W·m^{-2}) is the energy transferred per unit area, i.e., through the surface area perpendicular to the direction of flow. It is calculated by Fourier's law

$$q_x = -\lambda \frac{\partial T}{\partial x} \quad \text{Eq. 2}$$

In these particular models, the heat transfer from the clothing surface to the environment occurs from convection. This was modeled as

$$q = h \cdot (T - T_a) \quad \text{Eq. 3}$$

where h is the convection coefficient (W·m^{-2}·K^{-1}) and T_a is the air temperature (°C).

Boundary conditions

To set up the models, the initial skin temperature (T_s) was set to 31°C which is usually uncomfortably cold. The end node of the skin that did not touch the clothing was set to remain constant at 31°C. The skin temperature was fixed in the analysis, thus skin heat loss varied as the clothing changed. These changes in skin heat loss were the parameter assessed to determine how mass and temperature of the body armor increased or decreased the rate of body heat loss in the cold weather scenarios modeled in the experiment.

A separate boundary assessed was the interface where the clothing or armor meet the environment. Here there is heat transfer by convection, while conduction is negligible. This boundary was described by:

$$-\lambda \frac{\partial T}{\partial x} = h \cdot (T - T_a) \quad \text{Eq. 3}$$

where the h is dependent on wind speed [4], estimated by:

$$h = 10.4 \cdot v^{0.56} \quad \text{Eq. 4}$$

where v is wind speed in m·s^{-1}.

Initial Conditions

The dynamic simulations were executed with the assumption that the individual was initially in a warmed interior and in steady state with their clothing. They then don the body armor before stepping into the cold weather condition of the simulation. Thus negligible time was allowed to pass after donning the armor and entrance into the cold weather situation.

This dynamic simulation was performed with the armor added on top of the clothing and varied the initial temperature of the armor to simulate it being stored in warmed indoor situations and when stored in the ambient temperature of the outdoor environment. The skin and clothing were first simulated in static conditions where the ambient temperature was set at 20°C. The temperature of each mesh point on the clothing was then used as the initial temperature. While discontinuities in temperatures occur between the clothing layer and the armor and the armor and the ambient temperature, COMSOL Multiphysics® eliminates these gaps or discontinuities in the temperature between materials, creating a required continuous temperature across the displacement.

PARAMETERS

Thermal Properties

Material properties of each layer used in the simulations are shown in Table 1. Skin is a material built into COMSOL Multiphysics® and the default values within the software were used. The thermal conductivity of clothing was calculated based on resistance values of clothing measured on a thermal manikin. For the clothing and the outer layer of the IOTV, a thermal conductivity of 0.042 $W \cdot m^{-1} \cdot C^{-1}$ was used [3]. The ballistic insert material was assumed to be similar to Dupont Kevlar® 49 Aramid Fiber and the material properties were obtained online and these were used in the model [1]. The thermal properties of the ESAPI were either provided by NSRDEC or obtained through measurements. A thermal conductivity of 0.16 $W \cdot m^{-1} \cdot C^{-1}$ and a specific heat of 300 $J \cdot kg^{-1} \cdot K^{-1}$ was used [2]. The density of the ESAPI was obtained by using a scale to measure the mass and a 3D scan was performed with a GO!SCAN 3D™ (CREAFORM, Lévis,QC, Canada) which was then used to calculate the volume. The density of the ESAPI was then calculated by dividing the mass by the volume.

Table 1. Thermal properties of simulation materials

Material:	λ ($W \cdot m^{-1} \cdot K^{-1}$):	ρ ($kg \cdot m^{-3}$):	C_p ($J \cdot kg^{-1} \cdot K^{-1}$):
Skin	0.37	1109	3391
Clothing	0.042 [3]	1.20	1005
Ballistic Insert [1]	0.04	1440	1420
Outer Layer of IOTV	0.042 [3]	1.26	1005
ESAPI	0.16 [2]	1495	300 [2]

Geometry

The three models were created in one dimension with each material being represented by a layer with a calculated thickness. It was assumed that the skin was 2.5 mm thick [5]. The ESAPI was measured to be 25 mm thick by NSRDEC. All other thicknesses were estimated from the thermal resistances measured on thermal manikins using the empirical formula:

$$R = \frac{d}{\lambda} \qquad \text{Eq. 5}$$

where R is the resistance ($m^2 \cdot K \cdot W^{-1}$) and d is the thickness of the material layer (m). A typical unit used for thermal resistance is clo, which 1 clo is approximately equivalent to the thermal resistance of a business suit. Clo units can be converted to SI units by multiplying by a conversion factor of 0.155 $m^2 \cdot K \cdot W^{-1}$.

Table 2 shows the values used in calculating the thickness of each required layer of material for the simulations. One can use Eq. 5 to calculate the thickness of each layer. The thermal conductivity of the IOTV was calculated by taking the average thermal conductivity of the ballistic insert and outer layer because each layer made up half the thickness of the IOTV. The thickness of each layer calculated for the simulations are shown below in table 3.

Table 2. Resistances and thermal conductivities used to calculate the thickness of each layer.

Layer:	R (clo):	R ($m^2 \cdot K \cdot W^{-1}$):	λ ($W \cdot m^{-1} \cdot K^{-1}$):
Clothing (M1: clothing)	1.38	0.214	0.042 [3]
Clothing component of M2 (clothing+IOTV)	1.83	0.284	0.042 [3]
Clothing component of M3 (clothing+IOTV+ESAPI)	2.10	0.326	0.042 [3]
IOTV component of M2 (clothing+IOTV)	0.94	0.146	0.041
IOTV component of M3 (clothing+IOTV+ESAPI)	0.50	0.077	0.041

Table 3. Simulation interval thickness

	Thickness (mm)				
Model:	Skin:	Clothing:	Ballistic Insert:	ESAPI:	IOTV Outer Layer:
M1: clothing	2.5	9			
M2: clothing+IOTV	2.5	11	2.98		2.98
M3: clothing+IOTV+ESAPI	2.5	13.7	1.56	25	1.56

NUMERICAL METHODS

COMSOL Multiphysics® was used to compute the static and dynamic simulations. The simulations also contained parametric sweeps that were performed to determine the effect of varying a study parameter. Once complete, the heat flux from the skin was calculated within COMSOL Multiphysics® and was exported as a .csv file. The data was then imported into MATLAB® (Mathworks®; Natick, MA) for post processing.

In the steady state simulations $\frac{\partial T}{\partial t} = 0$. Thus the temperature at any point does not change over time and is constant.

In static conditions, one simulation was performed where T_a was set to values between 0 and -50°C, and wind speed set to 0.7 $m \cdot s^{-1}$. Another simulation was performed where the wind speed was varied. In this simulation, the T_a was set to -20°C and the wind speed was varied between 0.7 or 20 $m \cdot s^{-1}$.

Dynamic simulations were also performed. Now, $\frac{\partial T}{\partial t} \neq 0$. So, after the initial start point, the thermal balance changed, as was modeled with Eq.1, the heat transfer equation.

For dynamic conditions, the four simulations were:

A. T_a was set to values between 0 and -50°C and the wind speed was set to 0.7 $m \cdot s^{-1}$.

B. T_a was set to -20 °C and the wind speed was set to 0.7, 5, 10, and 15 $m \cdot s^{-1}$.

C. T_a was set to -20°C, the wind speed was set to 0.7 $m \cdot s^{-1}$, and the initial armor temperature was set to temperatures between 20°C and -20°C.

D. T_a was set to -40°C, the wind speed was set to 0.7 $m \cdot s^{-1}$, and the initial armor temperature was set to temperatures between 20°C and -20°C.

RESULTS

VALIDATION

Thermal manikin data with ensembles 1, 2 and 3 were used to validate the simulations. These experiments had the same clothing and equipment modeled as this report. The skin temperature (T_s) was 35°C, T_a was 20°C, and the wind speed was set to 0.7 $m \cdot s^{-1}$. The static heat flux values generated by COMSOL Multiphysics® were compared to heat flux measurements from the torso of the thermal manikin. The results are shown in Table 4.

Table 4. Heat flux results from simulations and thermal manikin experiments

T_s = 35°C, T_a = 20°C, Wind Speed = 0.7 $m \cdot s^{-1}$			
model	predicted heat flux ($W \cdot m^{-2}$)	measured heat flux ($W \cdot m^{-2}$)	error (%)
M1	44.45	45.88	-3.12
M2	26.21	27.86	-5.92
M3	22.00	29.30	-24.91

Differences between the simulations of M1 (clothing) M2 (clothing+IOTV) and experiments were < 6%; indicating that for these clothing situations the model assumptions and equations should acceptably simulate the environmental conditions tested with these clothing configurations. For M3, the predicted heat flux was unacceptably low relative to measured.

A second validation study was then performed. This time, a thermal manikin was placed in an environmental chamber and the heat flux was measured continuously throughout time. Clothing ensembles consistent with M2 (clothing+IOTV) and M3 (clothing+IOTV+ESAPI) were placed on the manikin. Next, T_s of the manikin was set to 35°C and T_a was initially set to 20°C. A steady state was reached and different heat fluxes were recorded throughout the manikin. In both validations, the conditions were modeled in COMSOL Multiphysics® by setting T_s to 35°C and creating a function in

MATLAB®, where T_a changed consistently with the recorded T_a around the manikin by using a linear interpolation function. Over the simulations it was assumed that the wind speed around the manikin was approximately 1 $m \cdot s^{-1}$.

In the M2 (clothing+IOTV) validation, the temperature was decreased to -20°C and then increased back to 20°C. The manikin measurements and COMSOL Multiphysics® predicted values are shown in figure 3. For validation of M3 (clothing+IOTV+ESAPI), the temperature was decreased to -20°C and later on it decreased to -40°C. The results are shown in figure 4. . Overall, the simulations appear to accurately model the actual outcome. The simulation of M2 (clothing+IOTV) precisely followed the measured heat flux of the manikin and is almost identical. In the simulation of M3 (clothing+IOTV+ESAPI), the heat flux appeared to lag behind the manikin heat flux. This could possibly be due to the simulations being 1 dimensional. In real life when the temperature suddenly changes, the clothing and IOTV would change temperature at a quicker pace than the ESAPI, which would create a heat flux that is not normal to the surface of the body as is assumed in a 1 dimensional simulation. However, the initial steady stat value appears to be identical and the approximate steady states at -20 and -40°C are close approximations.

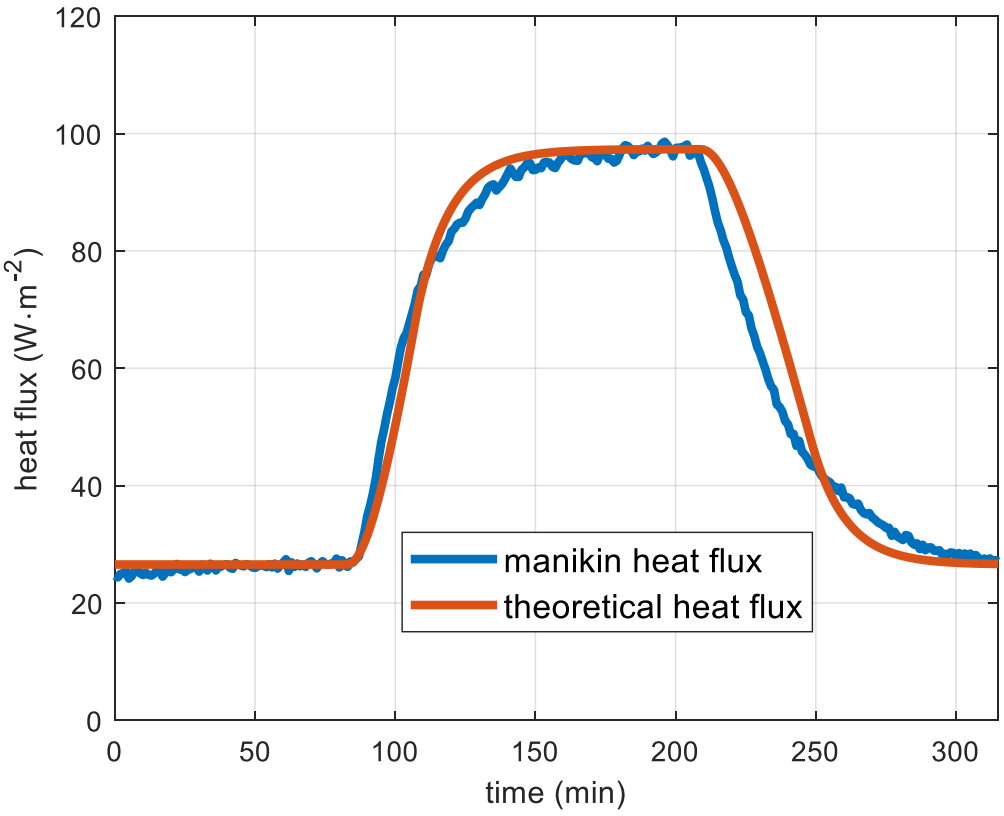

Figure 3: Measured and simulated heat flux with M2 (clothing+IOTV) when the ambient temperature changes from 20°C to -20°C

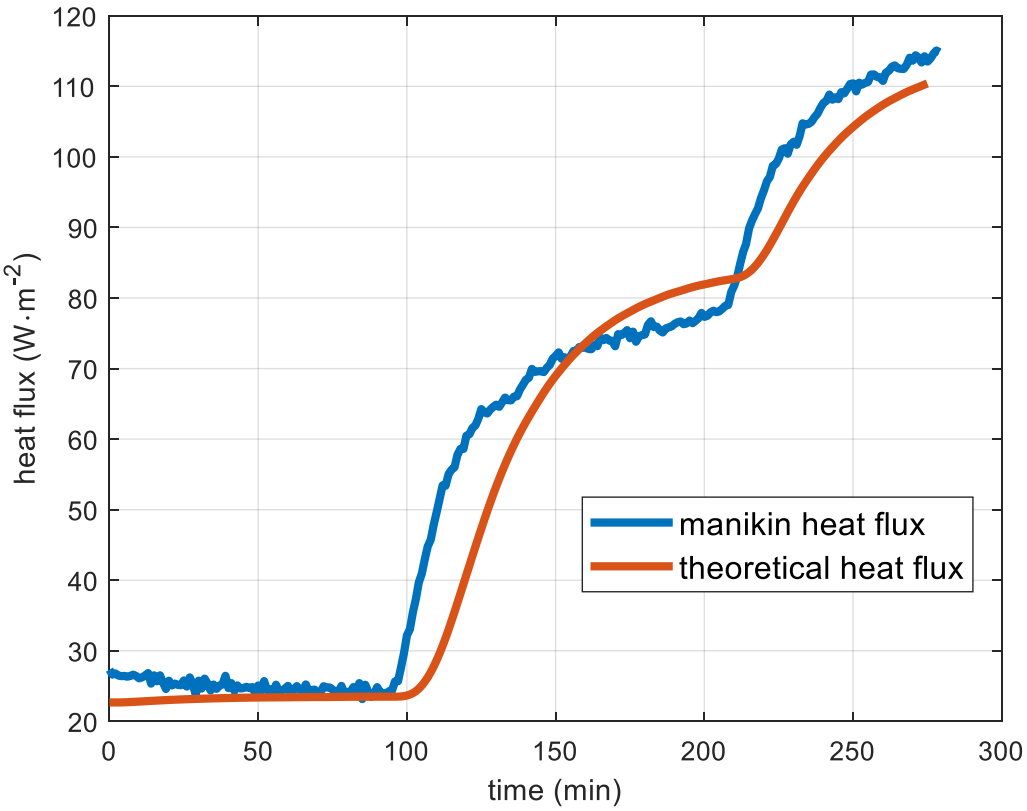

Figure 4: Measured and simulated heat flux with M3 (clothing+IOTV+ESAPI) when the ambient temperature changes from 20°C to -20C° and then from -20°C to -40°C

PREDICTIONS

STATIC SIMULATIONS

Figure 5 shows the differences in the static heat fluxes between the three models once steady state conditions were reached. The models show that the static heat flux of M1 (clothing) is greater than M2 (clothing+IOTV) and M3 (clothing+IOTV+ESAPI). However, the heat flux of M3 is less than M2, suggesting the addition of the ESAPI to the IOTV slightly decreases heat loss.

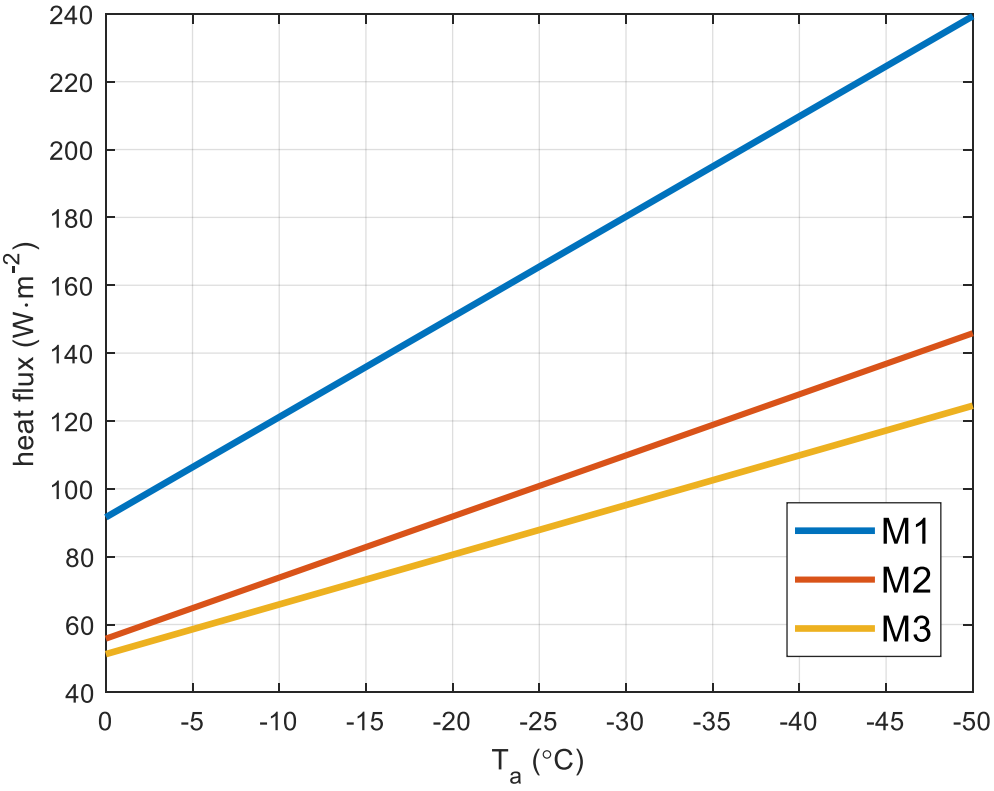

Figure 5: Static heat flux at skin layer when wearing M1 (clothing), M2 (clothing+IOTV), or M3 (clothing+IOTV+ESAPI) under different ambient temperatures and a wind speed of 0.7 $m \cdot s^{-1}$

Figure 5 shows how changing the wind speed affects the static heat flux of all three models. Overall the results show that when wind speed is increased, heat flux also increases. The change is non-linear with the largest increases in heat flux occurring between wind speeds of 1 to 6 $m \cdot s^{-1}$.

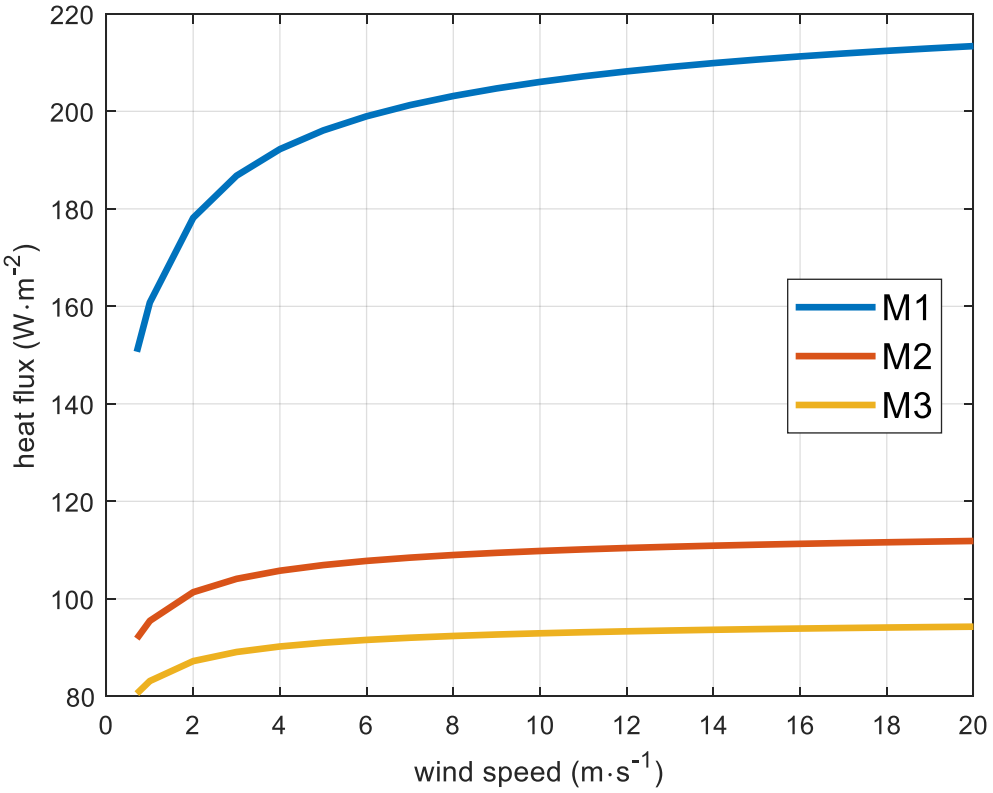

Figure 6: Static heat flux at skin when wearing M1 (clothing), M2 (clothing+IOTV), or M3 (clothing+IOTV+ESAPI), in ambient temperature of 20°C in multiple wind speeds

DYNAMIC SIMULATIONS

Figure 6 shows the heat flux changing over time when clothing and armor starts off in equilibrium at 20°C (~room temperature) and suddenly goes into an environment where T_a is 0, -20, -30, or -50°C. While all ensembles start off in a steady state, M1 (clothing) heat loss quickly increases and approaches a steady state in < 3 minutes. This is due to the low specific heat of clothing when modeled as air. In contrast, M2 (clothing+IOTV) and M3 (clothing+IOTV+ESAPI) are predicted to slow heat flux and to levels less than that of M1 (clothing).

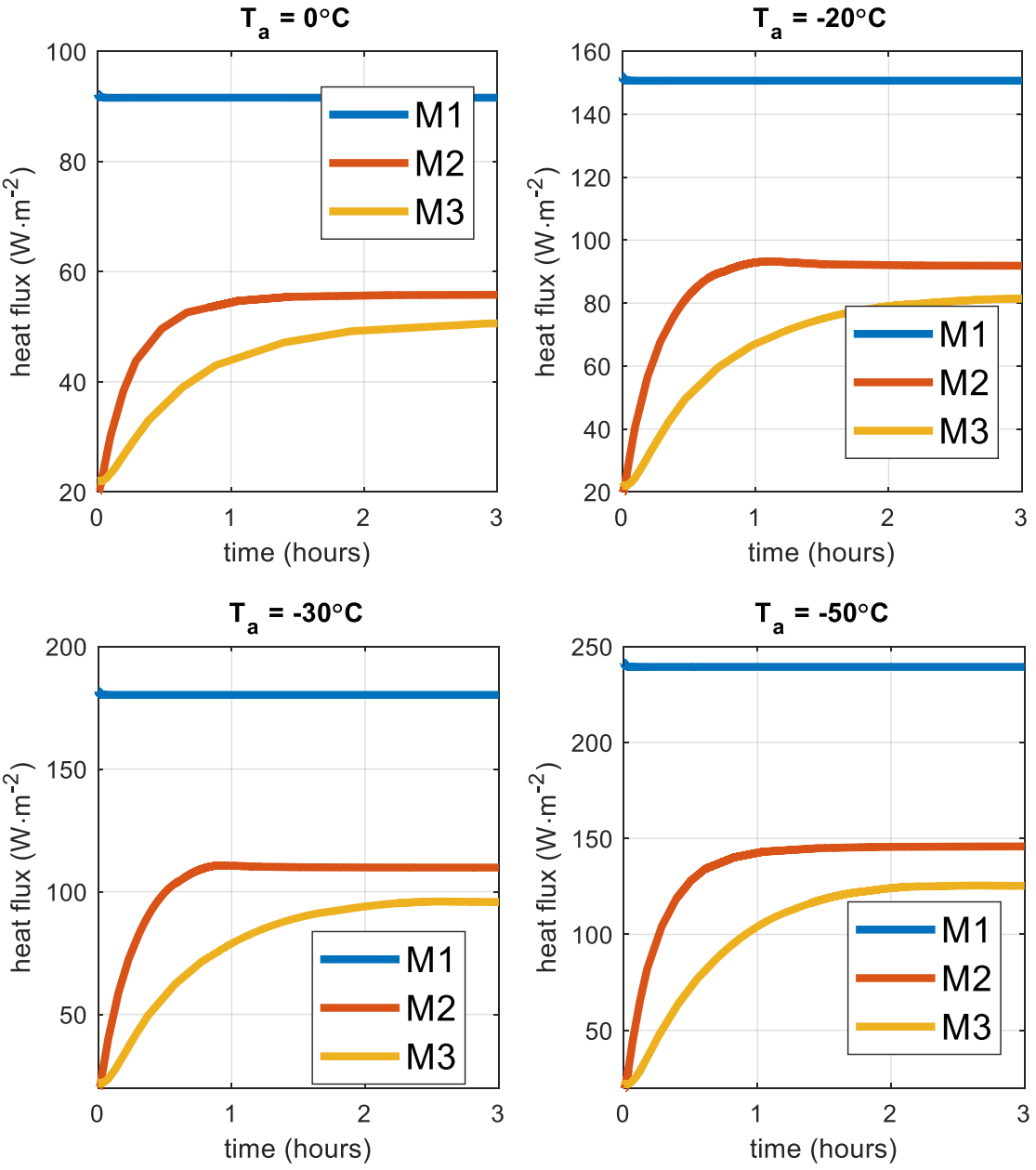

Figure 7. Heat flux at skin when wearing M1 (clothing), M2 (clothing+IOTV), or M3 (clothing+IOTV+ESAPI) when moving from indoor (20°C) to outdoor temperatures of 0, -20, -30, and -50°C and wind speed of 0.7m·s^{-1}

Figure 8 shows how the wind speed affects skin heat flux when wearing M1 (clothing), M2 (clothing+IOTV), or M3 (clothing+IOTV+ESAPI). The convection coefficient increases when the wind speed is increased. As a result the heat flux leaving the body is increased because more heat is lost due to convection with the environment. This increase is primarily due to an increase in wind speed from 0.7 to 5 $m \cdot s^{-1}$. Increasing the wind speed above 5 $m \cdot s^{-1}$ had a negligible effect on the heat flux. This is because h is proportional to $v^{0.56}$.

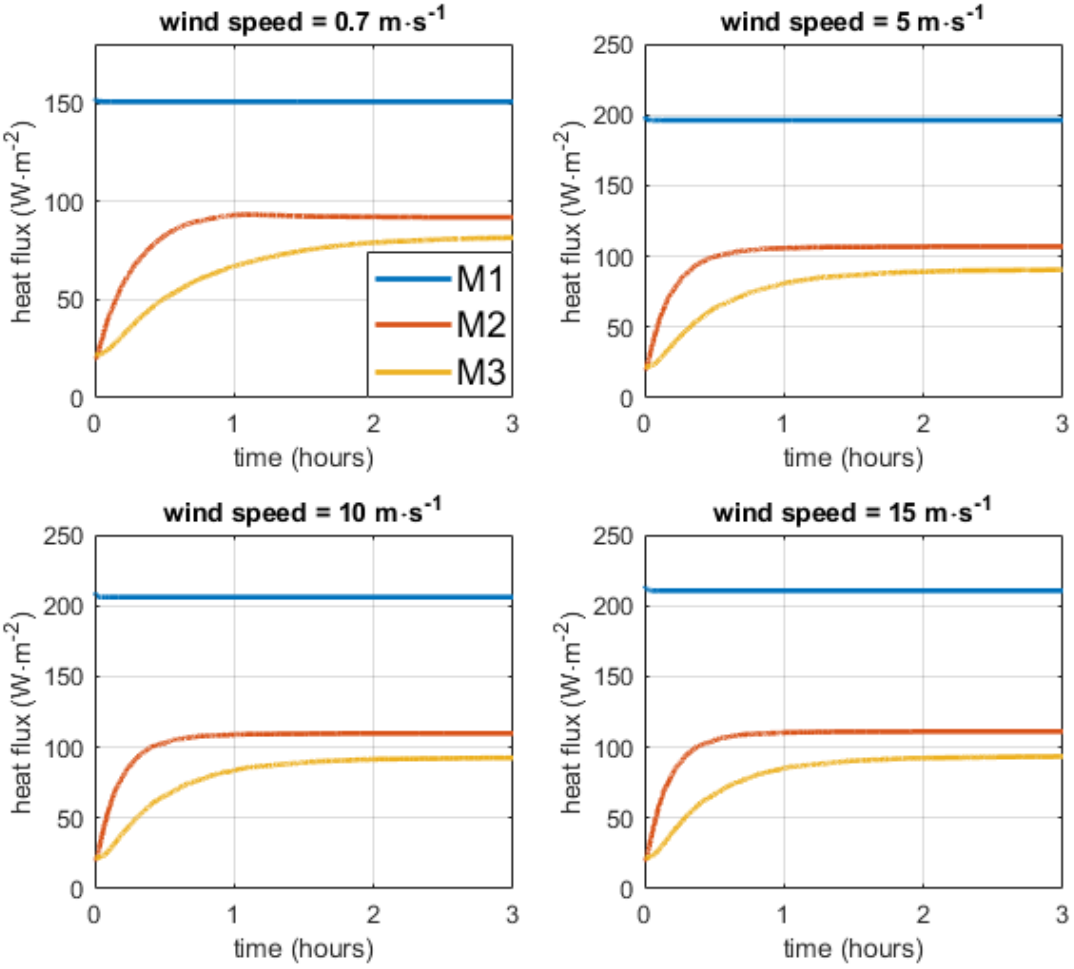

Figure 8: Heat flux at skin when wearing M1 (clothing), M2 (clothing+IOTV), or M3 (clothing+IOTV+ESAPI), and moving from indoor (20°C) to outdoor temperatures of -20°C and varying wind speeds

Figures 9 and 10 show how the initial temperature of the IOTV and ESAPI affects the heat flux at the skin when wearing M2 (clothing+IOTV) or M3 (clothing+IOTV+ESAPI). When the initial temperatures of the IOTV and ESAPI are reduced to simulate impact of donning them in cold weather, the heat flux is initially accelerated during the initial minutes of cold air exposure but then approaches the same static heat flux for that environmental situation. As shown in the results of M3 at -40°C, when the initial temperature of body armor was 20°C , the body heat loss was about 45 $W \cdot m^{-2}$ and then slowly increases to 110 $W \cdot m^{-2}$. However, when the initial temperatures of body armor was the environmental temperature, the heat loss was 200 $W \cdot m^{-2}$ and then slowly reduces to 110 $W \cdot m^{-2}$.

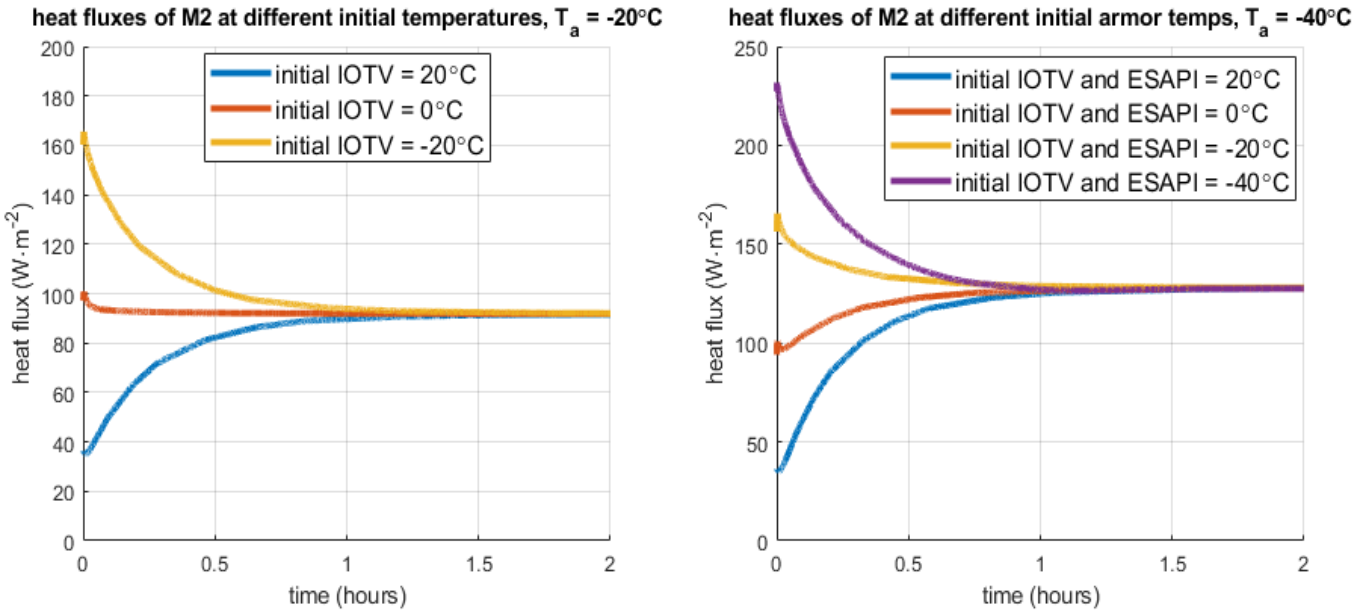

Figure 9. Heat flux at skin surfaces when wearing M2 (clothing+IOTV) with different initial temperatures and entering into T_a set at -20°C (left) and -40°C (right) with a wind speed of 0.7 $m \cdot s^{-1}$

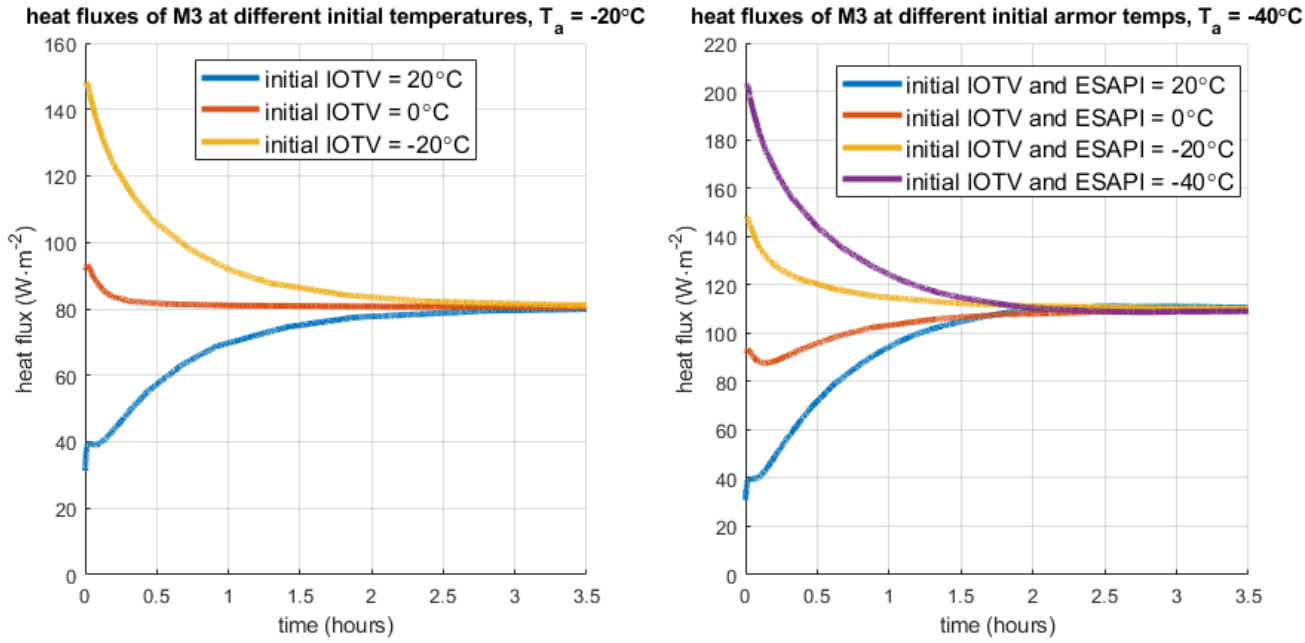

Figure 10: Heat flux at skin surfaces when wearing M3 (clothing+IOTV+ESAPI) with different initial temperatures and entering into T_a set at -20°C (left) and -40°C (right) with a wind speed of 0.7 m·s^{-1}

SENSITIVITY ANALYSIS

Sensitivity analysis was performed on the specific heat and density of the ESAPI. Figure 11 shows how changing the specific heat of the ESAPI affects the heat flux. When in a steady state, $\frac{\partial T}{\partial t} = 0$, which implies the value of C_p in Eq. 1 does not affect the steady state heat flux. In Figure 11, the C_p of the ESAPI is changed by ±10%. Throughout the entire simulation, the greatest difference in heat flux between a C_p of 330 J·kg^{-1}1·K^{-1} and a C_p of 270 J·kg^{-1}·K^{-1} is 2.54 W·m^{-2}, which takes place after 45 minutes. This corresponds to a percent difference of 2.58%, which is negligible.

Sensitivity analysis was also performed on the density of the ESAPI. The calculated density of the ESAPI is 1495 kg·m^{-3}. A dynamic simulation shows how the heat flux changes when the density is changed as well. In Figure 12, the density is changed by ±10%. The simulations show that the greatest difference in heat flux between the model with a density of 1445.5 kg·m^{-3} and the model with a density of 1644.5 kg·m^{-3} is 2.52 W·m^{-2} and occurs after 45 minutes. This corresponds to a percent difference of 2.58%, which is a negligible difference.

Sensitivity analysis was simulated by changing the thermal conductivity of the ESAPI by ±10%, however, this outcome is not shown because the change in the heat flux is negligible and the differences in the heat fluxes are indistinguishable when plotted.

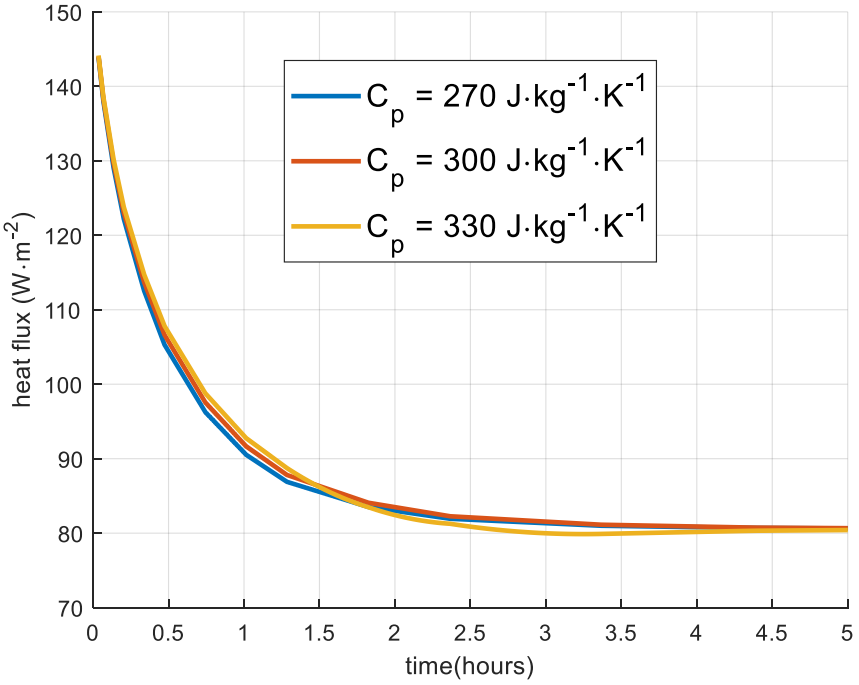

Figure 11. Heat flux at skin surface for different values of the ESAPI's Cp, when initial IOTV and ESAPI temperatures are -20°C, t_a = -20°C

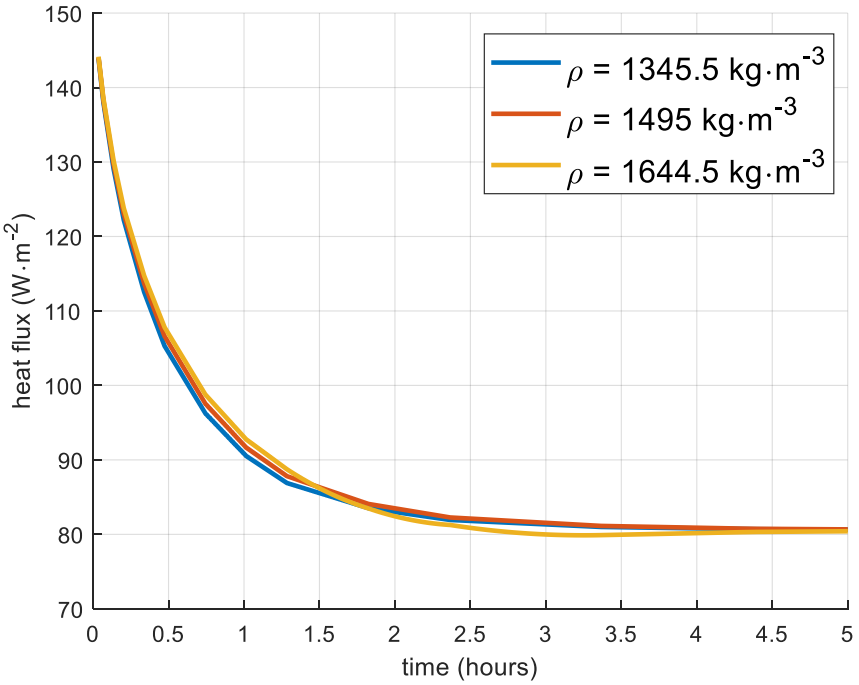

Figure 12: Heat flux at skin surface for different values of the ESAPI's density, initial IOTV and ESAPI temperature -20°C, t_a = -20°C

DISCUSSION

This report details the simulated effects of the IOTV and combined IOTV and ESAPI on body heat loss during exposure to cold environments. The results demonstrate that the IOTV adds insulation to the clothing system and reduces body heat loss in steady state conditions. However, the initial temperature of the IOTV impacts the rate of heat flux; when its initial temperature is warm the rate of body heat loss is slowed, and when it is cold it increases the rate of body heat loss. The practical implication is that that body armor stored in areas where temperatures are high, can slow body heat loss when doffed in cold weather.

The simulation approach was initially validated with data measured on a thermal manikin. This validation confirmed that the simulation approach produced acceptable estimates of heat flux. The simulation was then used to simulate the impact of wearing IOTV under varied cold weather conditions. This is the first research, to our knowledge to demonstrate how the IOTV affects body heat loss in cold environments. The simulations might be improved if more accurate measurements were available for each layer. Moreover, two dimensional or three dimensional simulations might increase accuracy, as these approaches would take into account special deformities at the interfaces between layers. Also, other elements like sweating and convection in large air layers between layers could be incorporated. However, there will always be a high degree of variance when studying clothing due to its stochastic behavior, such as the changes in thickness caused by movement or different body dimensions, or the air layers that can be within the clothing and armor system.

The accuracy of the one dimensional model could be improved upon by measuring the thickness of each layer with a material thickness gauge. This was not performed for the simulations because a gauge that would be able to measure the thickness in the torso region and not just the edge was not available. Instead resistances measured on a thermal manikin were provided. In using this approach, the clothing thickness of M2 (clothing+IOTV) and M3 (clothing+IOTV+ESAPI) were greater than that of M1 (clothing). Since the clothing would not actually increase thickness when armor is donned a simulation was performed where the clothing thickness was 9 mm for all three ensembles. As shown in Figure 13, when clothing thickness is held constant at 9 mm it takes approximately 10 minutes for the heat flux of M2 (clothing+IOTV) to become less than the heat flux of M1 (clothing) and 20 minutes for the heat flux of M3 (clothing+IOTV+ESAPI) to become less than the heat flux of M1(clothing).

We used the finite element method to solve and analyze heat flux during cold weather exposure. The COMSOL Multiphysics® software was selected as it does well at approximating differential equations. Without COMSOL Multiphysics® one could solve for Eq. 1 given initial temperatures, this would become extremely difficult or impossible when the dimensions are increased to two or three. The software and the simulation model employed allowed for examination of the dynamic heat flux events upon entry into multiple cold environments and the manipulation of the starting temperatures of the IOTV plates. This report demonstrates the relative impact of ambient temperature, wind,

and clothing/equipment temperatures on the predicted rate of heat flux and body heat loss when in moderate to extreme cold temperatures.

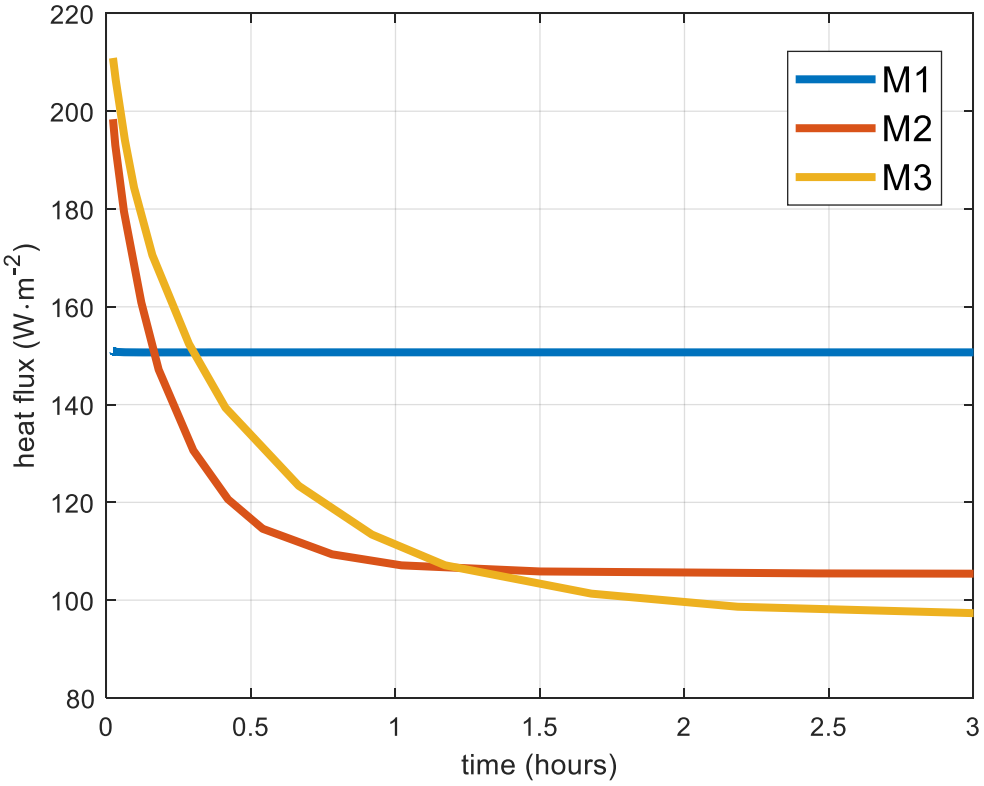

Figure 13: Heat flux at skin when wearing M1 (clothing), M2 (clothing+IOTV), or M3 (clothing+IOTV+ESAPI) when all clothing is 9 mm thick, T_a is -20°C, and the wind speed is 0.7 m·s^{-1}

CONCLUSIONS

This paper reports on simulated effects of the IOTV on body heat loss using finite element analysis. The simulation demonstrates how important the storage temperature of body armor can be, especially considering the ESAPI and IOTV may be stored in rooms in which the room temperatures may be as low as the outdoor environmental temperatures. Storing body armor in warm storage areas whenever possible will help prevent heat loss, especially during initial exposure periods to cold environments. This impact may last from 1 to 3 hours, depend on the storage temperature and outdoor environmental temperatures. When steady state is reached, however, body armor acts as a heat insulator and reduces body heat loss. The wind speed also plays a factor in how much heat is lost; with greatest dynamic effect from little to no wind to modest wind speed. At wind speeds above 5 m·s^{-1} the rate of heat flux is only modestly affected.

REFERENCES

1. Kevlar® Aramid Fiber Technical Guide. (n.d.). retrieved from http://www.dupont.com/content/dam/dupont/products-and-services/fabrics-fibers-and-nonwovens/fibers/documents/Kevlar_Technical_Guide.pdf
2. Auerbach, M., Proulx, G, Isherwood, K. (2017). Thermal Analysis of Armor System Materials, NSRDEC Internal Report
3. Xu X, and Werner J. A dynamic model of the human/clothing/environment-system. *Appl Human Sci* 16: 61-75, 1997
4. Xu, X., P. Tikuisis, P. (2014) Thermoregulatory modeling for cold stress, Comprehensive Physiology 4: 1057-1081. doi: 10.1002/cphy.c130047
5. Xu, X., T. R. Rioux, T. Macleod, T. Patel, M.N. Rome, and A.W. Potter (2017) Measured body composition and geometrical data of four "Virtual Family" members for thermoregulatory modeling International Journal of Biometeorology, 61 (3), pp 477–486.